

Electric Circuit Simulation of Floquet Topological Insulators

S. Sajad Dabiri¹ and Hosein Cheraghchi^{2,3,*}

¹Department of Physics, Shahid Beheshti University, 1983969411 Tehran, Iran

²School of Physics, Damghan University, P.O. Box 36716-41167, Damghan, Iran

³School of Physics, Institute for Research in Fundamental Sciences (IPM), 19395-5531, Tehran, Iran

(Dated: August 18, 2022)

We propose the simulation of every non-interacting time-periodic tight-binding Hamiltonian in electrical circuits with inductors and capacitors. First the time periodic Hamiltonian is mapped into a static Floquet Hamiltonian and so the time dimension is transformed into the Floquet dimension which in electric circuits is simulated as the additional dimension in space. However, the number of copies of the system which must be considered in this new dimension is controlled by the frequency and bandwidth. Furthermore, we show that the topological edge states (including anomalous edge states in the dynamical gap) can be detected in circuit by measuring the divergence of impedance between the nodes. Our results provide a simple and promising way to investigate and manipulate Floquet topological phases in electric circuits.

Introduction. Topological insulators (TIs) are materials which have insulating bulk but support conducting edge states [1, 2]. These edge states have a robust nature which cannot be removed by local perturbations which respect the protecting symmetries, so they are candidates for applications in various areas such as spintronic, quantum computation [3] and etc. Albeit, materials with intrinsic topological properties are limited and it is desirable to find a route to induce topological properties in various materials. An extension of TIs are Floquet TIs which are obtained by applying time-periodic perturbations such as terahertz laser fields irradiated on trivial or topological insulators [4], semimetals [5] and other systems.

Although the Floquet TIs seem a promising candidate for investigating the topological phenomena and moreover as a platform to make new topological states without counterpart in static systems [6], they are experimentally hard to realize and manipulate in condensed matter systems due to some problems such as heating which may cause melting of the sample. Furthermore, dissipation mechanisms in contact with reservoirs can destroy the Floquet states [7], which are inevitable in experiments of solid state systems.

Recently it has been shown that topological properties can be realized in metamaterials like electrical circuits. This includes the realization of TIs [8], topological semimetals and also higher order TIs [9]. Since the fabrication of such systems are easy and they are controllable, and also they do not suffer from undesired effects such as lattice imperfection and interaction with environment and etc., they are good candidates for investigating the topological properties.

In this paper we propose to simulate every non-interacting time-periodic (Floquet) tight binding Hamiltonian in electrical circuits with inductors and capacitors. By Fourier decomposition, we map the time peri-

odic Hamiltonian into a static Hamiltonian and then explain its implementation in electric circuits. The dimension of the circuit of the driven system will be effectively one more than the static time-averaged one. Nonetheless, the number of nodes which must be considered in the new direction (called Floquet direction) is approximately limited for finite bandwidth and frequencies.

Floquet formalism : Floquet theorem is a powerful tool in studying the time periodic systems. Suppose the time periodic Hamiltonian $H(t) = H(t + T)$, where T is the time period, (we set $\hbar = 1$) then Floquet theorem suggests the form of the solution of Schrodinger equation in the form of $|\psi_\alpha(t)\rangle = e^{-i\varepsilon_\alpha t}|\phi_\alpha(t)\rangle$ where the Floquet quasi modes are time periodic $|\phi_\alpha(t + T)\rangle = |\phi_\alpha(t)\rangle$, α is the band index and ε_α is the quasienergy which is defined modulo $\Omega = 2\pi/T$. The first Floquet Brillouin zone for quasi energies is defined as $(-\Omega/2, \Omega/2)$. For simplicity, let us convert Schrodinger time-dependent equation into a time-independent one by means of Fourier transformation, albeit at the expense of increasing the dimension of the Hilbert space. Using the Floquet Ansatz for eigenvalues of Schrodinger equation, we derive $[H(t) - i\partial_t]|\phi_\alpha(t)\rangle = \varepsilon_\alpha|\phi_\alpha(t)\rangle$. Since Hamiltonian and Floquet quasi-modes are time-periodic, Schrodinger equation in Fourier space is obtained as [10]

$$\mathbf{H}_F \phi_\alpha = \varepsilon_\alpha \phi_\alpha \quad (1)$$

where

$$\mathbf{H}_F = \begin{pmatrix} \ddots & \vdots & \vdots & \vdots & \ddots \\ \cdots & H^0 - \Omega & H^1 & H^2 & \cdots \\ \cdots & H^{-1} & H^0 & H^1 & \cdots \\ \cdots & H^{-2} & H^{-1} & H^0 + \Omega & \cdots \\ \ddots & \vdots & \vdots & \vdots & \ddots \end{pmatrix} \phi_\alpha = \begin{pmatrix} \vdots \\ |\phi_\alpha^1\rangle \\ |\phi_\alpha^0\rangle \\ |\phi_\alpha^{-1}\rangle \\ \vdots \end{pmatrix} \quad (2)$$

Where $H^n = \frac{1}{T} \int_0^T H(t) e^{in\Omega t} dt$ and $|\phi_\alpha^n\rangle = \frac{1}{T} \int_0^T |\phi_\alpha(t)\rangle e^{in\Omega t} dt$. The Floquet Hamiltonian in Eq. 2 is an infinite dimensional, Hermitian, static

* cheraghchi@du.ac.ir

Hamiltonian. The eigenvalues of \mathbf{H}_F are formed as the quasi-energy bands which are periodic in energy. Indeed, all bands which lie in the first Floquet zone are copied in other Floquet side bands. The quasi-energy interval $((m-1/2)\Omega, (m+1/2)\Omega)$ shows the band width of m th Floquet side band. Fortunately infinite dimensional Floquet Hamiltonian represented in Eq. 2 can be truncated for a system with finite bandwidth to give an approximate solution. As noted in Refs. [11, 12] the effect of m th side band i.e. $\langle \phi_\alpha^m | \phi_\alpha^m \rangle$ is highly suppressed for $|m| > \ell_m = \mathcal{W}/\Omega$. The \mathcal{W} is the bandwidth which may be taken as $\mathcal{W} = \max(|H^n|)$ for $n \in \mathbb{Z}$.

One can visualize the Floquet Hamiltonian in Eq. 2 as a combination of time averaged Hamiltonians, which have different onsite potentials (Ω is the difference of onsite potential between nearest neighbours) which are coupled to each other with H^n , ($n \neq 0$) [13] where H^n can be viewed as coupling between the n th neighbours. If the static Hamiltonian H^0 is a tight binding version with dimension d , then Floquet Hamiltonian can be considered as a tight binding Hamiltonian with an extra dimension i.e. $d+1$.

Let us discuss two limiting cases. First in high frequency regime $\Omega \gg \mathcal{W}$, the Floquet side bands are effectively decoupled, known as Wannier-Stark localization [13], and the effect of n th side band ($n \neq 0$) can be applied perturbatively on the zeroth side band. In this regime the topology of the system is described by Altland-Zirnbauer (AZ) classes [14] for static systems in d dimension [15]. On the other hand, if $\Omega \ll \mathcal{W}$, we are in adiabatic regime, then all Ω s in Eq. 2 can be neglected, and the topology of the system is described by the static AZ classes in $d+1$ dimension [15]. Indeed beyond these two limits, the topological classification is different from static systems and shows rich features [16, 17].

Circuit construction: In electrical circuits, the Kirchhoff's law yields the relation between currents and voltages [8, 9, 18]

$$\dot{I}_p = \sum_q C_{pq}(\ddot{V}_p - \ddot{V}_q) + \frac{1}{L_{pq}}(V_p - V_q) + C_p \ddot{V}_p + \frac{V_p}{L_p} \quad (3)$$

Where $\dot{\square} = \partial_t \square$, and I_p (V_p) is the current entering from the external source (voltage) at the node p , C_p (L_p) is the capacitance (inductance) between the node p and the grounded electrode, moreover, C_{pq} (L_{pq}) is the capacitance (inductance) between the node p and the node q . For a voltage mode, $V(t) = V(0)e^{i\omega t}$ with frequency of ω , it is written as

$$I_p(\omega) = \sum_q J_{pq}(\omega)V_q(\omega) \quad (4)$$

In the above formula, $J(\omega) = \sum_n j_n |\chi_n\rangle \langle \chi_n|$ is the grounded Laplacian of the circuit and j_n , $|\chi_n\rangle$ are its

eigenvalues and eigenvectors. Laplacian is defined as [18]

$$\begin{aligned} J_{pq}(\omega) &= i\omega(t_{pq}(\omega) + \delta_{pq}\mu_p(\omega)) \\ t_{pq}(\omega) &= -C_{pq} + \frac{1}{\omega^2 L_{pq}} \\ \mu_p(\omega) &= C_p - \frac{1}{\omega^2 L_p} - \sum_\nu t_{p\nu} \end{aligned} \quad (5)$$

One can find a relation between the circuit Laplacian and a tight binding Hamiltonian. If we write $J_{pq}(\omega) = i\omega H_{pq}$, then H_{pq} can be considered as a tight binding Hamiltonian, in which $t_{pq}(\omega)$ is the hopping between sites p and q , and $\mu_p(\omega)$ denotes the onsite potential at site p . The nodes play the role of sites in the lattice. In this picture, capacitors are equivalent to negative hopping parameters. The positive hoppings can be simulated by inductors $-C \leftrightarrow \frac{1}{\omega^2 L}$ or by considering a subnode [18]. In Ref. [18], it was shown that a hopping with an arbitrary complex phase can be simulated by the subnode method. Alternatively, the complex hoppings can be implemented with operational amplifiers [19]. One of the main measurable quantities is impedance between nodes which is written as [8, 9]

$$\begin{aligned} Z_{pq} &= G_{pp} + G_{qq} - G_{pq} - G_{qp} \\ &= \sum_n \frac{|\chi_{n,p} - \chi_{n,q}|^2}{j_n} \end{aligned} \quad (6)$$

Where $G = J^{-1}$ is the Green function of the circuit. To find the two-point impedance experimentally, the two nodes should be attached to an external current source, so a current such as I_p exits from the p node and enters into another node, let's call it q . Then the impedance is derived as the ratio of the potential difference between these two nodes and the current at the p node; $Z_{pq} = \frac{V_p - V_q}{I_p}$ [20]. It was shown that the impedance diverges between the edges of the sample in a topological phase due to the localization of wave functions of edge states and vanishing j_n [8, 9]. Interestingly, the Green's function of the circuit can be determined experimentally by entering a current through the p node I_p and measuring the potential at the q node, $V_q^{(p)}$, so the Green's function is defined as $G_{pq} = \frac{V_q^{(p)}}{I_p}$ [21]. Moreover, the band structure of the system is accessible in experiment [22]. If the Floquet Hamiltonian is considered as a static tight binding with $d+1$ dimension, then this Hamiltonian can be simulated in electrical circuits which consist of capacitors and inductors [18]. In the following we demonstrate this possibility and try to implement Floquet Hamiltonian in an electrical circuit for a simple model.

Driven SSH circuit: The Su-Schrieffer-Heeger (SSH) model firstly was proposed for electronic states in polyacetylene [23]. It is a tight binding Hamiltonian in one dimension with two atoms in unit cell and intracell (in-

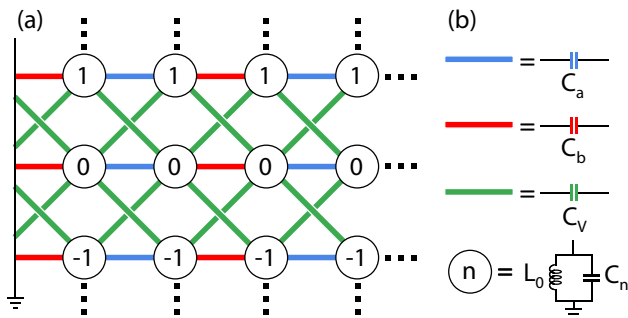


FIG. 1. (a) The driven SSH circuit. Each row shows a static SSH circuit with capacitors C_a, C_b . They are connected with capacitor C_V which plays the role of drive. Different rows have different groundings (corresponding to chemical potential in tight binding Hamiltonian). (b) The meaning of elements used in part (a).

tercell) hopping parameters $t_a(t_b)$. In real space it reads

$$H_{SSH} = \sum_j t_a c_{a,j}^\dagger c_{b,j} + t_b c_{b,j-1}^\dagger c_{a,j} + h.c. \quad (7)$$

where $c_{a,j}^\dagger (c_{a,j})$ creates and destroys a particle on site j in the sublattice a . For $|t_a/t_b| < 1$ ($|t_a/t_b| > 1$), the model is in topological (trivial) phase. Circuit simulation of this model shows that there exists an impedance divergence between the ends of the chain in the topological phase [8]. If we modulate the hopping parameters in a time-periodic manner, then the topological characterization of the model is different from the static one [24]. The edge states may disappear or be created by variation of the frequency and intensity of the drive. Interestingly for on-resonant drive (with a frequency lower than the band width) edge states may appear at the dynamical gap at quasienergies $\pm\Omega/2$ which can not exist for static systems.

We modulate the hopping parameters of the SSH model in the following manner $t_{a,b}(t) = t_{a,b} + 2V \cos(\Omega t)$, to achieve the driven SSH model. In the k space, the time-dependent Hamiltonian can be written as

$$H(k, t) = \begin{pmatrix} 0 & t_a(t) + t_b(t)e^{-ik} \\ t_a(t) + t_b(t)e^{ik} & 0 \end{pmatrix} \quad (8)$$

We intend to make the circuit version of the Floquet Hamiltonian in Eq. 2 for driven SSH model. Fig. 1 (a) shows this circuit and Fig. 1 (b) the meaning of elements of (a). It consists of several static SSH circuits (rows with capacitors $C_a = -t_a$ and $C_b = -t_b$) with different groundings, which are connected by the capacitors $C_V = -V$. Each node is denoted by a numbered circle indicating the grounding of that node. The nodes in the n^{th} row are grounded by an inductor L_0 and capacitor C_n . We assume that $C_n - C_{n-1} = \Omega$. It should be noted

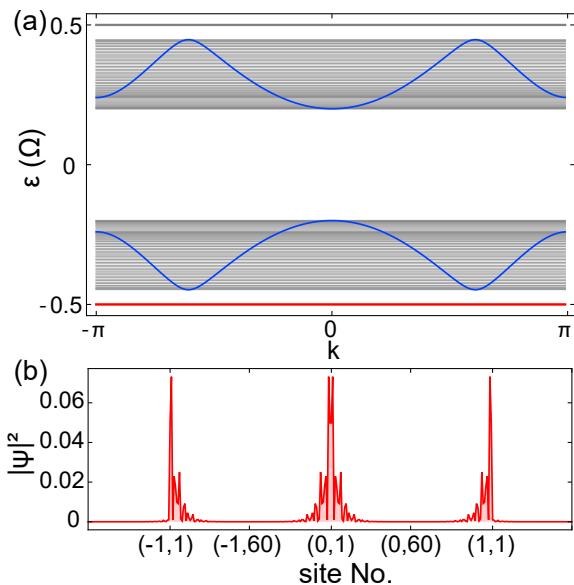


FIG. 2. (a) The quasienergy dispersion of a driven SSH model with parameters $t_a = -1.3, t_b = -0.7, V = -0.3, \Omega = 2.5$. Blue lines show the bulk band structure with periodic boundary condition whereas the gray and red lines show the band structure with open boundary condition (120 sites in each row is used). (b) The square of the wave function of the midgap state at quasienergy $-\Omega/2$ which is depicted in part (a) by red color. It is seen that this midgap state is localized at the edges of the sidebands 0, -1.

that the total conductances exiting from a node in n^{th} row are $i\omega(C_a + C_b + 4C_V + C_n - \frac{1}{L_0\omega^2})$.

The topological nature of driven SSH model can be determined by evaluating the Zak phase [24] in the following way: the Floquet Hamiltonian must be truncated to the dimensions which guarantees the convergence of the results, then to check the existence of an edge mode in a gap, Zak phases of all bands below the gap must be added up. Zak phase of each band can be calculated numerically by summing the relative phases of wave functions in a discrete Brillouin zone. On the other hand, one can check the number of edge modes in open boundary condition. Consider the driven SSH model with $t_a = -1.3, t_b = -0.7, V = -0.3, \Omega = 2.5$. In this case there is one resonance in band structure between 0^{th} and $\pm 1^{\text{th}}$ side bands. It is obvious that the non driven case with such parameters is in the trivial phase which hosts no zero state. On the contrary, the driven model hosts midgap states at quasienergy $\pm\Omega/2$. The sum of the Zak phases of bands of Floquet Hamiltonian, below quasienergy 0 ($\Omega/2$) is equal to 0 (π) modulo 2π . The band structure of Floquet Hamiltonian is shown in Fig. 2 (a). The blue lines correspond to bulk states with periodic boundary condition and gray or red lines to the system with open boundary condition (with 120 sites). Red lines show the midgap states for which the square of wavefunction is plotted in Fig. 2 (b). It is seen that

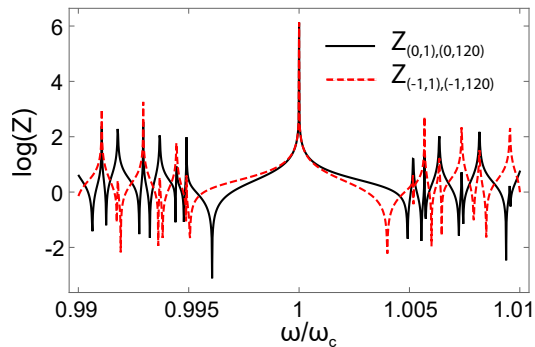


FIG. 3. The impedance between the ends of the 0^{th} (-1^{th}) row, which is specified by black (red dashed) color. The circuit parameters are $C_a = 1.3, C_b = 0.7, C_V = 0.3, C_{-4} = \Omega/2, C_n - C_{n-1} = \Omega, L_0 = (C_A + C_b + 4C_V + 4\Omega)^{-1}, \Omega = 2.5$

the wave function is mainly localized at the edges of the -1^{th} and 0^{th} sidebands, because this midgap state is a consequence of a resonance between these two sidebands. The wave functions of midgap states decay exponentially to the bulk with an exponent which is proportional to the associated gap [24]. Nonetheless, by increasing the amplitude of the drive, the midgap states' wave function will have non negligible amount on the edges of the other side bands too, albeit this effect is highly suppressed for side bands which are farther from -1^{th} and 0^{th} sidebands.

Because of the localization of the midgap states, they may be tracked by impedance measurement in circuit simulation. Since the midgap state shown by the red line in Fig. 2 is pinned to the quasienergy $-\Omega/2$, we set the grounding in a way to move it to zero quasienergy in order to have a divergence in impedance. In our numerical calculations we retain $(2 \times 4 + 1) = 9$ side bands. So we set $C_{-4} = \Omega/2, C_n - C_{n-1} = \Omega$, and $L_0 = (C_a + C_b + 4C_V + 4\Omega)^{-1}$. Then from Eq. 6, we expect that at frequency of $\omega_c = 1$ there is a divergence for impedance between the ends of the chain in -1 and 0 rows. We assume that there are 120 sites at each row. Fig. 3 shows the impedance $Z_{(0,1),(0,120)}$ which is between the nodes $(0, 1)$ and $(0, 120)$, where the first (second) component specifies the number of sideband (the site number in each row). Also $Z_{(-1,1),(-1,120)}$ is depicted by the red dashed line in this figure. The divergence in impedance occurs at the frequency $\omega_c = 1$ which is clearly seen in Fig. 3. We also checked that this divergence also occurs for $Z_{(-1,1),(0,120)}$ at ω_c but not for $Z_{(-1,1),(0,1)}$ or $Z_{(-1,120),(0,120)}$.

Now consider the limits of high and low frequencies. In the high frequency limit $\Omega \gg \mathcal{W}$, it is sufficient to consider the effect of side bands perturbatively on the zeroth side band. Then we can define an effective Hamiltonian in one dimension which captures the topology of the system. If $U(T)$ denotes the evolution operator of the system in a period, then $U(T) = \mathcal{T} \int_0^T e^{-iH(t)} dt = e^{-iH_{\text{eff}}T}$. There are some expansions of this effective Hamiltonian in inverse powers of frequencies known as vanVleck and

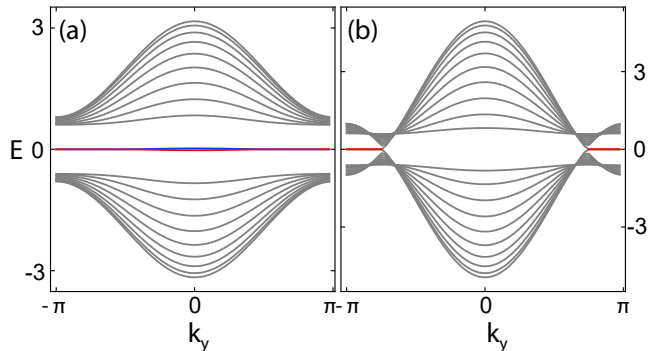


FIG. 4. Dispersion relation of nanoribbon version of Hamiltonian in Eq. 9 for the parameters (a) $t_a = 0.7, t_b = 1.3, 2V = 0.6$ and (b) $t_a = 1.3, t_b = 0.7, 2V = 1.5$ with open (periodic) boundary condition along $x(y)$.

Brillouin-Wigner expansions [25]. If the effective Hamiltonian H_{eff} is topologic and have a nontrivial winding number, then the model shown in Fig. 1 will have zero modes localized mostly at the ends of the zeroth row.

On the other hand, in the low frequency regime $\Omega \ll \mathcal{W}$ one can set the groundings in Fig. 1 identically for all nodes, i.e. $C_n = 0$. Assuming $\Omega t \rightarrow k_y, k \rightarrow k_x$, the Hamiltonian in this adiabatic regime can be written as

$$H_{\text{adia}}(k_x, k_y) = [t_a + 2V \cos(k_y) + (t_b + 2V \cos(k_y)) \cos(k_x)] \sigma_x + [t_b + 2V \cos(k_y)] \sin(k_x) \sigma_y \quad (9)$$

This model is very similar to the zigzag Graphene model introduced in Ref. [8]. Although the Chern number of this model is zero due to time reversal symmetry, this model can have nearly flat band edge states which can be detected with impedance measurements, showing a large impedance at the edges of the sample [8].

The nearly flat edge states are present (absent) when $|\frac{t_a + 2V \cos k_y}{t_b + 2V \cos k_y}| < 1$ ($|\frac{t_a + 2V \cos k_y}{t_b + 2V \cos k_y}| > 1$) due to the winding number of one dimensional model. See Ref. [26] for topological arguments about these nearly flat edge states. We draw the band structure of the nanoribbon version of the Hamiltonian of Eq. 9 for the parameters $t_a = 0.7, t_b = 1.3, 2V = 0.6$ ($t_a = 1.3, t_b = 0.7, 2V = 1.5$) in Fig. 4 a (b) respectively. The edge states are shown with the red and blue colors. Clearly, the former case is an insulator with flat edge states in all momenta and the latter is a semimetal with flat edge states in some range of momenta $|k_y| > \arccos(-2/3)$.

Conclusion. In summary, we have shown that every non interacting tight binding Floquet Hamiltonian can be simulated in electrical circuits. The method is based on simulating the Floquet Hamiltonian in Fourier space, which leads to an extra dimension for circuits compared with the static system. It is shown that the n^{th} Fourier component of time-periodic Hamiltonian, corresponds to

n^{th} neighbour coupling in Floquet direction, so the circuits with one harmonic mode will be more easily constructed. The number of needed copies of the system in the extra direction is controlled by the bandwidth and frequency of the drive. For higher frequencies and lower

bandwidths, the number of these copies can be small. We showed that the intrinsically dynamical edge states in driven systems can be detected by a divergence in impedance between edges of the sample. Our work paves the way for studying and detecting the Floquet topological phases in experimental setups.

-
- [1] M. Z. Hasan, C. L. Kane, *Rev. mod. phys.*, 82, 3045 (2010).
- [2] Y. Ando, *J. Phys. Soc. Japan*, 82, 102001(2013).
- [3] F. Wilczek, *Nat. Phys.*, 5, 614-618(2009).
- [4] N. H. Lindner, G. Refael, V. Galitski, *Nat. Phys.* 7.6 490 (2011).
- [5] T. Oka and H. Aoki, *Phys. Rev. B*. 79, 081406 (2009).
- [6] M. S. Rudner, N. H. Lindner, E. Berg, M. Levin, *Phys. Rev. X*, 3, 031005 (2013).
- [7] S. A. Sato, U. De Giovannini, S. Aeschlimann, I. Gierz, H. Hübener, A. Rubio, *J. Phys. B*, 53, 2251201 (2020).
- [8] C. H. Lee, S. Imhof, C. Berger, F. Bayer, J. Brehm, L. W. Molenkamp, T. Kiessling, R. Thomale, *Communications Physics*, 1, 1-9 (2018).
- [9] S. Imhof, C. Berger, F. Bayer, J. Brehm, L. W. Molenkamp, T. Kiessling, F. Schindler, C. H. Lee, M. Greiter, T. Neupert, R. Thomale, *Nature Physics*, 14, 925-929 (2018).
- [10] T. Kitagawa, T. Oka, A. Brataas, L. Fu, and E. Demler, *Phys. Rev. B* 84, 235108 (2011).
- [11] M. S. Rudner, N. H. Lindner - arXiv preprint arXiv:2003.08252. (2020)
- [12] N. H. Lindner, E. Berg, M. S. Rudner, *Phys. Rev. X* 7, 011018 (2017).
- [13] T. Oka, S. Kitamura, *Annu. Rev. Condens. Matter Phys.*, 10, 387-408 (2019).
- [14] A. P. Schnyder, S. Ryu, A. Furusaki and A. W. W. Ludwig, *Phys. Rev. B* 78, 195125 (2008).
- [15] A. Gómez-León, G. Platero, *Phys. Rev. Lett.*, 110, 200403(2013).
- [16] R. Roy, F. Harper, *Phys. Rev. B*, 96, 155118 (2017).
- [17] S. Yao, Z. Yan, Z. Wang. *Phys. Rev. B*, 96, 195303 (2017).
- [18] J. Dong, V. Juričić, B. Roy, *Phys. Rev. Research*, 3, 023056 (2021).
- [19] T. Hofmann, T. Helbig, C. H. Lee, M. Greiter, R. Thomale, *Phys. Rev. Lett.* 122, 247702 (2019).
- [20] S. M. Rafi-Ul-Islam, Z. B. Siu, C. Sun, M. B. Jalil, *New J. of Phys.*, 22, 023025 (2020).
- [21] T. Hofmann, T. Helbig, F. Schindler, N. Salgo, M. Brzezinska, M. Greiter, T. Kiessling, D. Wolf, A. Vollhardt, A. Kabaši, C. H. Lee, A. Bilušić, R. Thomale, T. Neupert, *Phys. Rev. Research*, 2, 023265 (2020).
- [22] T. Helbig, T. Hofmann, C. H. Lee, R. Thomale, S. Imhof, L. W. Molenkamp, T. Kiessling, *Phys. Rev. B*, 99, 161114 (2019).
- [23] W. P. Su, J. R. Schrieffer, A. J. Heeger, *Phys. Rev. Lett.* 42, 1698 (1979).
- [24] V. Dal Lago, M. Atala, L. F. Torres, *Phys. Rev. A*, 92, 023624 (2015).
- [25] T. Mikami, S. Kitamura, K. Yasuda, N. Tsuji, T. Oka, H. Aoki, *Phys. Rev. B*, 93(14), 144307 (2016).
- [26] M. Ezawa, *New J. Phys.*, 16, 115004 (2014).